Ⓔ

Rayleigh-Wave H/V via Noise Cross Correlation in Southern California

by Jack B. Muir and Victor C. Tsai

Abstract   We study the crustal structure of southern California by inverting horizontal-to-vertical (H/V) amplitudes of Rayleigh waves observed in noise cross-correlation signals. This study constitutes a useful addition to traditional phase-velocity-based tomographic inversions due to the localized sensitivity of H/V measurements to the near surface of the measurement station site. The continuous data of 222 permanent broadband stations of the Southern California Seismic Network (SCSN) were used in production of noise cross-correlation waveforms, resulting in a spatially dense set of measurements for the southern California region in the 1–15 s period band. The fine interstation spacing of the SCSN allows retrieval of high signal-to-noise ratio Rayleigh waves at periods as low as 1 s, significantly improving the vertical resolution of the resulting tomographic image, compared to previous studies with minimum periods of 5–10 s. In addition, horizontal resolution is naturally improved by increased station density. Tectonic subregions including the Los Angeles basin and Salton trough are clearly visible due to their high short-period H/V ratios, whereas the Transverse and Peninsular Ranges exhibit low H/V at all periods.

Electronic Supplement: Maps of horizontal-to-vertical (H/V) ratios and their standard deviation, and the count of H/V ratio measurements exceeding the signal-to-noise ratio requirements and tables of the numbers used for the maps, along with figures of inverted V_S and a Markov chain Monte Carlo histogram.

Introduction

The development of noise cross-correlation techniques constitutes one of the major developments of observational seismology in the past 15 years (Shapiro and Campillo, 2004). As a result of the many possible pairs of stations in a seismic network such as the Southern California Seismic Network (SCSN) ($n(n − 1)/2$ independent pairs for a network of n stations) and the lack of dependence on earthquake source location, noise cross correlation delivered a level of data density that was unprecedented little more than a decade ago.

The fundamental result of the noise cross-correlation technique is that cross correlating an ambient noise wavefield between two points results in a signal approximately proportional to the causal and anticausal far-field Green's function between those two points (Snieder, 2004; Boschi and Weemstra, 2015). Practically, waveforms approximating the displacement Green's function between two seismic stations can be constructed by correlating noise traces (of length sufficient to capture the phase of interest) at each station in the time domain, and then stacking them to produce an average (Bensen *et al.*, 2007).

The power spectral density of seismic noise is at a maximum in the 5–20 s period band, as a result of the primary and secondary oceanic microseisms at peak periods of 15 and 7 s, respectively (Ardhuin *et al.*, 2015). The dominance of oceanic noise also means that the global noise wavefield is primarily generated near the Earth's surface. Consequently, the seismic mode best observed in noise cross-correlation measurements is the short-period fundamental-mode Rayleigh wave, as it is well excited by surface noise sources in this period band.

Generally, it has been thought that Rayleigh waves are more easily observed in noise cross correlation than Love waves, as *P–SV* motion is excited at the Earth's surface at a greater rate than *SH* motion. Cross-correlation studies have therefore focused heavily on Rayleigh-wave techniques, especially the traditional measurements of phase and group velocities for tomographic imaging (Shapiro, 2005), although some studies have shown that Love waves may be clearly observed (Lin *et al.*, 2008). As the cross-correlation technique matures, amplitude information derived from noise cross-correlation studies has begun to supplement velocity measurements.

Absolute amplitudes of noise cross correlations, or even relative interstation amplitudes, are difficult to interpret theoretically due to the differing effects of real noise distributions
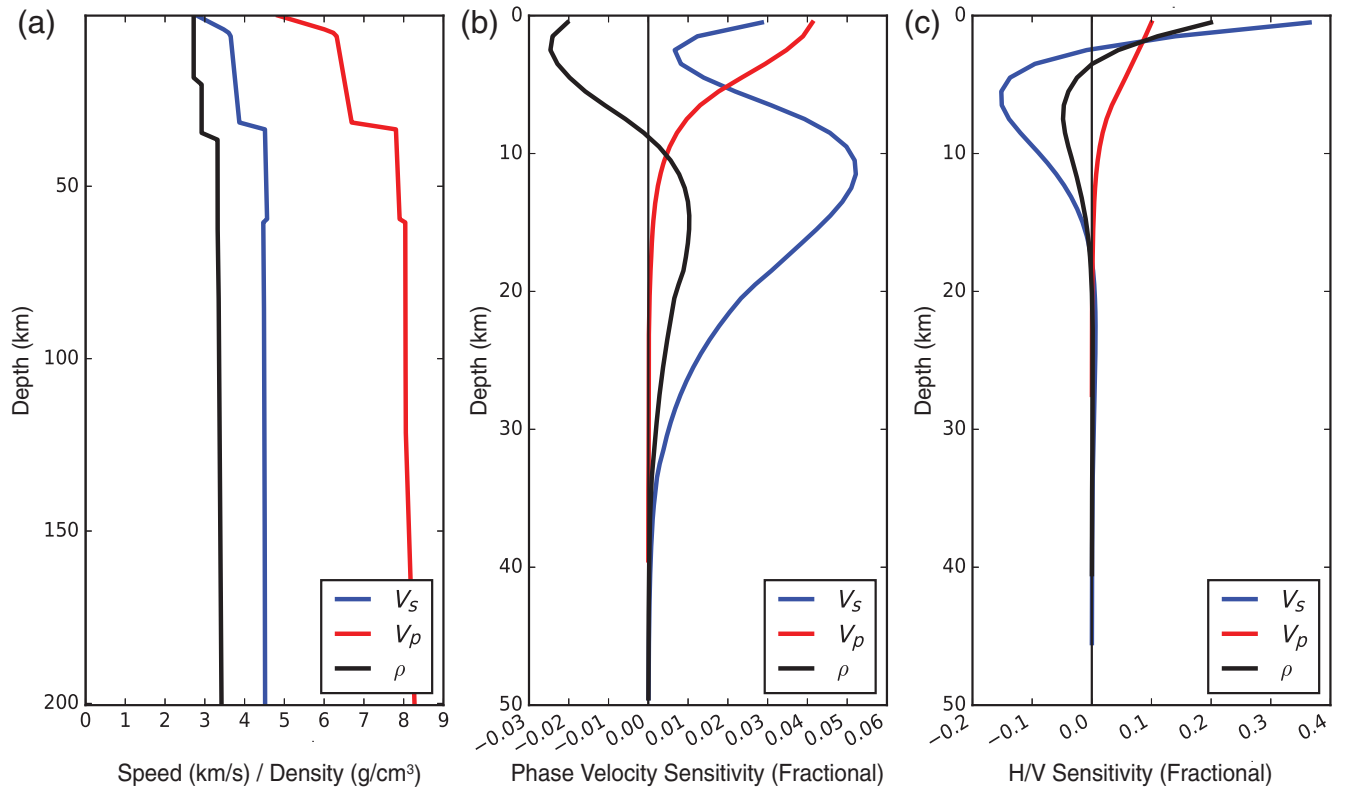
Figure 1.   (a) Southern California Hadley–Kanamori 1D velocity model for P-wave velocity (V_P), S-wave velocity (V_S), and density (ρ) to a depth of 200 km. (b) Rayleigh-wave phase velocity sensitivity to perturbations in V_P, V_S, and ρ at depth at a period of 10 s. (c) Rayleigh-wave horizontal-to-vertical (H/V) sensitivity to perturbations in V_P, V_S, and ρ at depth at a period of 10 s.

(e.g., Tsai, 2011); however, the amplitude ratios between noise cross-correlation components are more robust due to common noise source and wave propagation, particularly if care is taken to jointly, rather than independently, normalize all components (Lin *et al.*, 2014). We note that noise cross-correlation derived horizontal-to-vertical (H/V) match earthquake H/V in their overlapping period range, providing empirical evidence of the robustness of the noise derived H/V (Lin *et al.*, 2014). Similarly to traditional event waveform H/V amplitude ratios of Rayleigh waves, H/V of noise cross correlations are highly sensitive to upper crustal structure in the immediate vicinity of the receiving station.

H/V ratios derived from single-station noise power spectral densities have the advantage of being easy to derive from even short deployments. However, it is difficult to definitively interpret single station measurements; they have been variously interpreted in terms of Rayleigh waves (Boore and Toksöz, 1969; Fäh *et al.*, 2001), vertically propagating *SH* waves (Nakamura, 2000), or diffuse-wave theory (Sánchez-Sesma *et al.*, 2011). The method presented here does not suffer from this theoretical uncertainty. The use of noise cross-correlation traces instead allows for clear identification of Rayleigh waves by observation of elliptical particle motion and windowing of seismograms around the expected Rayleigh-wave arrival time. Hence, H/V ratios derived from noise cross correlations may be interpreted using Rayleigh-

wave forward modeling. H/V ratios are especially sensitive to basin structures, in which the large impedance contrast between the basin material and underlying bedrock results in a characteristically peaked H/V spectrum, exhibiting a basin resonance effect.

Figure 1 shows that Rayleigh-wave H/V sensitivity is concentrated at the near surface, relative to the sensitivity of Rayleigh-wave phase velocities for the Hadley–Kanamori 1D velocity model of the Transverse Ranges, which is commonly used as a reference velocity model for southern California (Hadley and Kanamori, 1977; Hutton *et al.*, 2010). Sensitivity is even greater close to the surface for models containing low-velocity basins, as the eigenfunction amplitudes become sharply peaked in the basin at resonant frequencies. This high surface sensitivity, with suppressed sensitivity at depth relative to phase-velocity measurements, makes Rayleigh-wave H/V ratios an exciting prospect for highly vertically resolved tomographic studies of the near surface.

In this study, we employed the regionally dense permanent SCSN to observe H/V values in southern California. Southern California is an ideal test site for new seismic methodologies because it is simultaneously structurally complex and well studied. Thus, there is a wealth of comparisons that can be made with previous results. Cutting-edge tomographic results in especially complex regions such as the Los Angeles basin rely on joint inversion for many seismic

observables, up to and including full waveform inversions for which the forward problem is prohibitively expensive for many applications and a high-quality initial 3D model is required. In comparison, ambient noise cross correlation is relatively inexpensive, with good results available after only a several-months-long deployment of a small broadband network. H/V tomography (e.g. Lin *et al.*, 2012, 2014; Li *et al.*, 2016) utilized noise cross correlations and long-period Rayleigh waves in a combined period band of 8–100 s. The 8–100 s period band results in good vertical resolution at a continental scale and combined with phase-velocity measurements is sensitive to the whole crust; however, it does not contain the short-period data necessary to image the upper 10 km of the crust at kilometric length scales. Expanding the period range of Rayleigh-wave H/V via noise cross-correlation techniques to a minimum period of 1 s should therefore prove especially useful in maximizing the utility of preliminary regional crustal studies, where events during station deployment are limited and the regional crustal model is of poor resolution.

Methodology

Three-component broadband (BH channel) data were obtained for the year 2015, for 222 permanent stations of the SCSN. The data were divided into 1 hr segments. The data were then preprocessed using the methods described in Bensen *et al.* (2007), with the following modifications: To facilitate efficient computation, the data were decimated from their natural sampling rate of 40 Hz to 5 Hz after being low-pass filtered to prevent aliasing. The cutoff for the low-pass filter was 2.5 Hz, well above the 1 Hz maximum frequency used for computing H/V ratios for this study, and so did not affect the reported results. For each station, all three components were normalized in the time and spectral domains using a common normalization signal, to maintain the relative amplitude information necessary for H/V ratio measurement; in contrast to coherency measurements of amplitude this method allows for a meaningful measurement of amplitude ratios. The common signals used to normalize the time and spectral domain records were taken to be the means of the single component signals for each channel, as described in Bensen *et al.* (2007).

H/V ratio measurements were then performed following Lin *et al.* (2008). Nine-component cross correlations between all station pairs were calculated for each hour; the resulting cross correlations were then stacked for all available hours in 2015 to produce the final hour-long averaged traces. To calculate H/V ratios, the cross correlations were rotated from the measurement (east–north–vertical [ENZ]) frame into the radial–transverse–vertical (RTZ) frame between the two stations, and then filtered to the period of interest using a Butterworth band-pass filter. To simultaneously rotate all nine components into the correct RTZ frames, the rotation matrix may be simply calculated as $\mathbf{M} = \mathbf{M}_1 \otimes \mathbf{M}_2$, in which $\mathbf{M}_{1,2}$ are the three-component rotation matrices from the ENZ to the RTZ frame for the individual stations and $\otimes$ is the Kronecker product. This calculation extrapolates to the case of a general 3D rotation (see Laub, 2005, chapter 13). We also calculated empirically derived back azimuths from ZR/ZT particle-motion ellipses to account for any effect ray path bending away from the great-circle arc may have on the calculated H/V ratios. Using the empirical back azimuths increased the H/V ratios by a maximum of 10% in the 3–5 s period band; however, as rotation by the empirical back azimuths did not appear to substantially improve the calculated waveforms, we report only the great-circle path-rotated results here.

To avoid misidentifying higher-mode Rayleigh waves as the fundamental mode of interest, the theoretical arrival times of the fundamental mode and first overtone were calculated, and the signal before the mean of these times removed. The phase gradient of the identified peak was logged to record the sense of motion of the arrival. As noted by Tanimoto and Rivera (2005), the sense of motion is period dependent and may switch from retrograde to prograde for the fundamental mode in the presence of steep surface-velocity gradients, which can complicate the identification of the fundamental mode. As a result, further discrimination between potential first overtone and fundamental-mode signals was not performed using the phase gradient. Furthermore, record sections of the calculated noise cross correlations do not show coherent moveout of the first overtone. The root mean squared amplitude of the waveform near the maximum of the envelope of each component was then used to make amplitude ratio measurements between components. Example waveforms, with the time intervals used for the calculation of H/V intervals highlighted, are shown in Figure 2.

Once the H/V values for each station pair were collected, quality control was further performed by removal of low (<15) signal-to-noise ratio (SNR) measurements, with the last 100 s of the causal cross correlation taken as the noise reference. The four components of interest in calculating H/V ratios (out of the nine calculated components) are ZZ, ZR, RZ, and RR, in which the first letter corresponds to the component of the source and the second to the receiver for the causal cross-correlation signal (i.e., ZR corresponds to a vertical impulse at the virtual source being recorded on the radial component of the receiver). Both ZR/ZZ (initial vertical impulse) and RR/RZ (initial radial impulse) H/V measurements may be made; however, as the RR component of the causal cross correlation failed the SNR criterion at a much higher rate than ZZ and ZR, the RR/RZ H/V values are not reported in this study. For each receiver station, each virtual source that satisfied the SNR criterion was used to generate summative H/V spectra. The ZR/ZZ H/V measurements are approximately lognormally distributed; for the purposes of inverting for velocity structure, we assume that they follow a lognormal distribution at each period, for each receiver. Interstation spacing varies widely throughout the SCSN, with the densest spacing in the Los Angeles basin. As H/V is principally dependent only on structure local to the receiver, the station density should not influence the
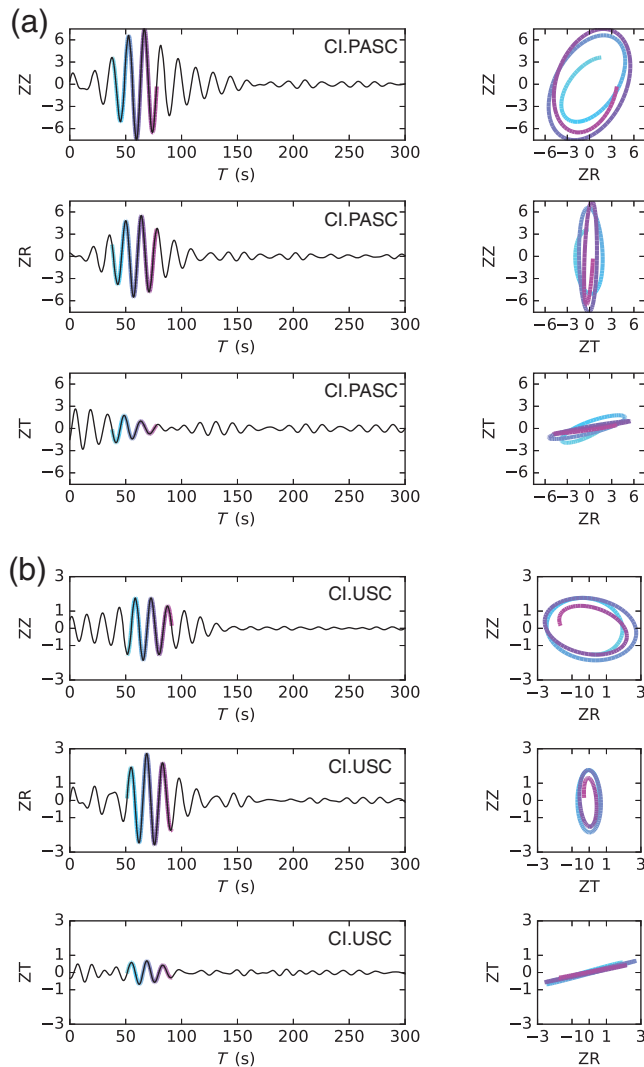
Figure 2. Waveforms and particle motions, filtered to a central period of 5 s, for (a) a hard-rock site (Pasadena Arts Center [PASC], signal-to-noise ratio [SNR] of 92) and (b) a basin site (University of Southern California [USC], SNR of 73). The colored area shows the time interval used for H/V calculation.

inversion results, with the possible exception of fewer short-period data in regions with low station density, as the amplitude of short-period waves decay rapidly with distance.

The resultant log H/V spectra were then used to invert for 1D near-surface structure underneath each of the available SCSN stations using the genetic algorithm global function minimizer provided by MATLAB (see Data and Resources). A 1D average velocity model for southern California provided by the Southern California Earthquake Center was used as the initial parametrization (Hutton *et al.*, 2010). This smoothed initial parametrization captures some of the efforts of previous tomographic results, without overly conditioning the prior information. Theoretical H/V values were calculated using the finite-element method of Lysmer (1970) to solve for Rayleigh-wave fundamental-mode eigenfunctions. The structure was parametrized by five layers

(0–500, 500–1000, 1000–2000, 2000–4000, and 4000–8000 m), with the V_P/V_S and V_P/ρ ratios set by the empirical relationships of Brocher (2005). This parametrization was chosen because five layers was the minimum required to fully fit the observed H/V peaks; the increasing layer thicknesses with depth helps avoid overspecification of the forward model; however, the choice of parametrization was ultimately subjective.

Results and Discussion

Figure 3 shows an example of the median of the collected H/V results, in this case for central periods of 2 and 7 s. The median H/V, standard deviation of the H/V logarithms, and the counts exceeding SNR at each station at all periods from 1 to 15 s are available in Ⓔ Figures S1–S45 (available in the electronic supplement to this article). There are tables of data containing all recorded amplitudes and SNRs available as Ⓔ Tables S1–S3. Major sedimentary basin regions of southern California (the Los Angeles basin and the Salton trough) are clearly visible as regions of elevated H/V ratios, particularly in the 2–8 s period band. Basins with smaller land surface expressions (Ventura basin, Santa Maria basin) and with fewer deployed seismometers (Central Valley) are also visible on a limited selection of stations. We expect the H/V ratios at each station to be closer to lognormal than normal in distribution (as the amplitudes are a product of many positive multiplicative factors). Maps of the standard deviation of the H/V logarithms show little correlation with known structures, other than a general increase within the Los Angeles basin (see Ⓔ Figs. S31–S45). It is difficult to speculate on the underlying cause behind the differing variance in H/V ratios, as it does not show consistent trends with either values of the H/V ratio, number of measurements exceeding the SNR criterion, the back azimuth to the source station, distance to the ocean (the predominant noise source at most periods), or station density.

Figure 4 shows two examples of H/V spectra as a function of period exhibiting typical hard-rock and basin site features. The H/V spectra are generally well fit by a five-layer parameterization for nearly all stations. There is significant trade-off between basin depth and near-surface velocity within inversions; however, fitting both the width and amplitude of the H/V peak, if present, does allow for basin depth and velocity to be independently resolved. Figure 5 shows the inverted V_S maps for the top two layers of the parametrization that result from the use of the measured ZR/ZZ H/V ratios. Basin structures are clearly observable within the inverted V_S model as regions of depressed velocity persisting several kilometers into the crust. We performed an ensemble Markov chain Monte Carlo (MCMC) inversion of the vertical velocity profile underneath the University of Southern California (CI.USC) to assess the uncertainties in the inversion results (see Ⓔ Fig. S51) using the *emcee* Python package, which natively handles the nonlinear and highly correlated likelihood surface of the forward problem (Foreman-Mackey *et al.*,
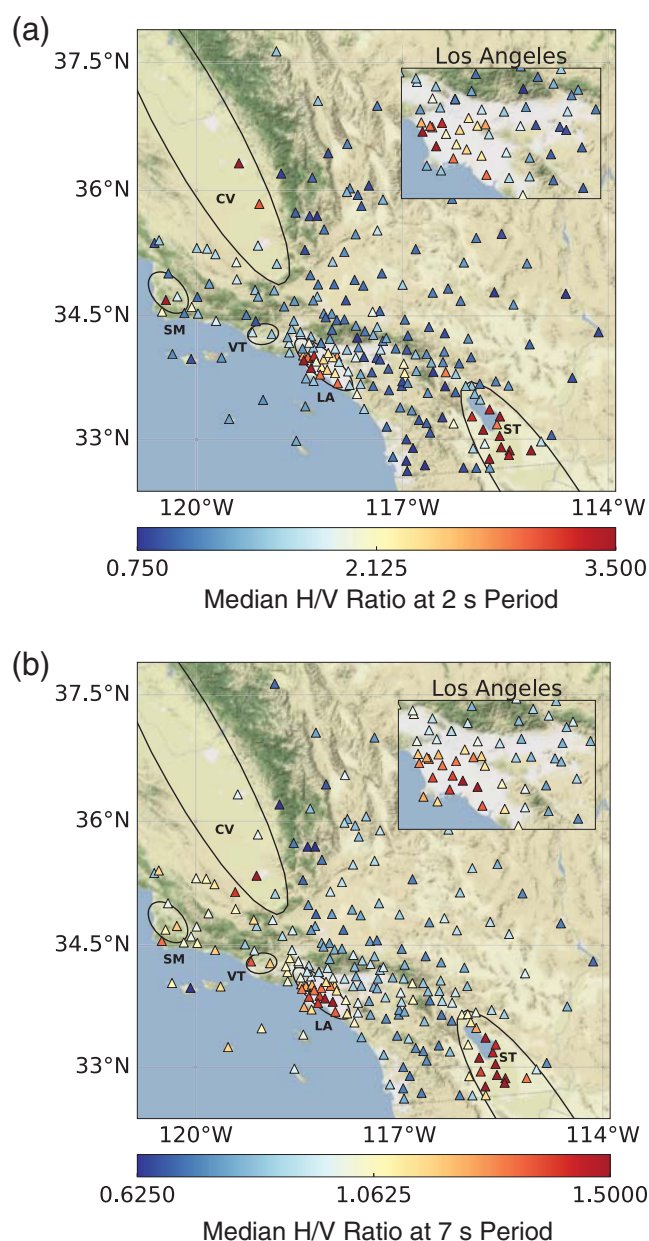
Figure 3. H/V aggregate measurements using the ZR and ZZ cross-correlation components at central filtering periods of (a) 2 s and (b) 7 s. Inset plots show the Los Angeles basin area; note the different color scales for each subplot.

2013). The results show increased confidence in the inversion of the near-surface parameters, as expected from the sensitivity behavior of H/V ratio measurements. The extensive computational requirements of the MCMC sampling process preclude us from performing this analysis for all stations.

A notable inference that can be made from Figure 5 is that inversions based on H/V ratios suggest a shallower effective basin depth (in the sense of horizontal seismic amplification) than is currently defined within the southern California Community Velocity Models (CVMs), of which we use the Harvard CVM (CVM-H; Shaw *et al.*, 2015). Ma and Clayton (2016), using Rayleigh- and Love-wave

dispersion along the Los Angeles Syncline Seismic Interferometry Experiment also found a shallower layer of very low velocities in the Los Angeles basin than that contained in the CVM-H basin, although their deep velocity structure is more similar to the CVM-H than ours. The theoretical H/V ratios predicted by the CVM-H model are shown in Figure 4 as dashed black lines; for the CI.USC station example the CVM-H predicts a larger amplitude and longer period than found in the empirical data. The mismatch between H/V ratios predicted by CVM-H and those measured empirically is frequent within basin areas; as can be seen in the Pasadena (CI.PASC) station example, in hard-rock sites the spectra are quite flat and there is not as strong evidence for potential mismatches within the period range studied here. Matsushima *et al.* (2014) and others invoked nonplanarity of subsurface interfaces to explain similar discrepancies between observations and theory in microtremor H/V ratio data, and obtained similarly reduced amplitudes and shorter periods. However, the effect they observed is significantly weaker than the mismatches between CVM-H predicted H/V and the H/V we observed. Additionally, the effect of nonplanar interfaces (and anisotropic velocity) should be apparent as an azimuthally dependent H/V ratio, for which there is only weak evidence in our dataset. Further exploration of this effect requires a large-scale numerical simulation of ambient noise propagation within southern California and is therefore outside the scope of this article.

Conclusions

We obtained noise cross-correlation-derived measurements of Rayleigh-wave H/V ratios for the SCSN in the 1–15 s period band. Robust statistics are obtained for the majority of stations, showing clearly elevated H/V ratios within the major basin regions of southern California within the 2–8 s period band. The H/V ratios have been inverted also for 1D profiles of V_S beneath the recording stations.

These results confirm the ability of dense seismic arrays to produce useful H/V measurements at shorter periods than in the optimally excited oceanic microseism period band. Recorded patterns of H/V ratios correlate very well with known structure in southern California throughout the period range studied. These results provide a useful additional constraint on near-surface structure that may be folded into large collaborative models such as the CVM-H, even within their high-resolution basin zones, and could potentially improve near-surface resolution within the less studied areas of the southern California region. Within this study, the use of a single theoretical framework (surface-wave inversion) results in a self-consistent map of V_S, unlike existing CVMs that are often nonphysically discordant as a result of resolution changes across the model according to data availability. Furthermore, the good concordance with known structure validates the use of short-period H/V measurements to develop detailed near-surface crustal models underneath other
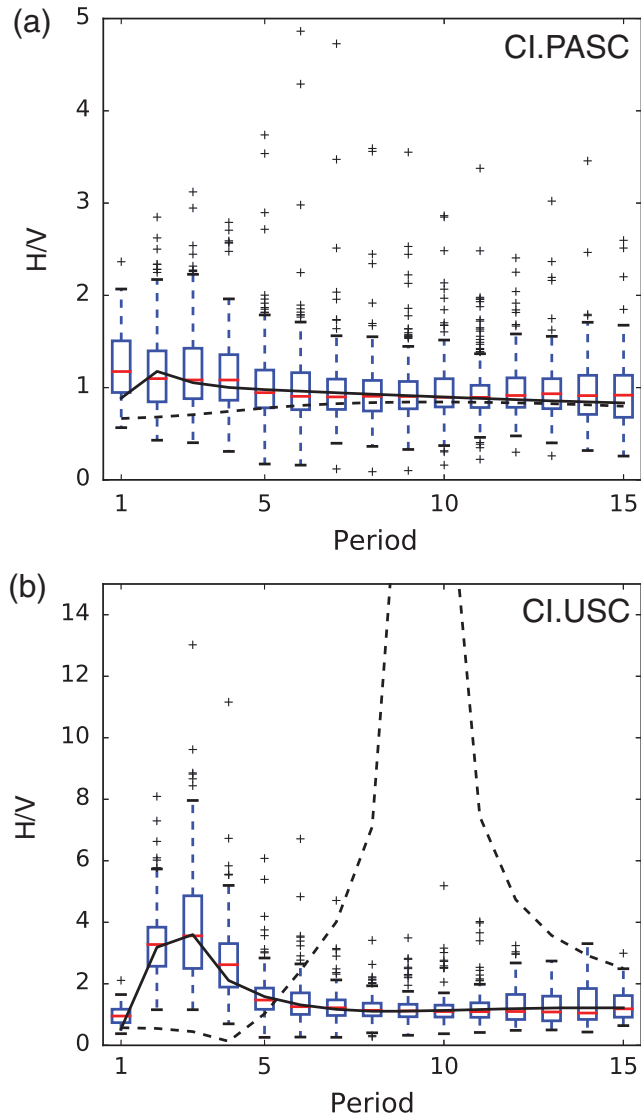
Figure 4. Example boxplots of H/V spectra with lines from fitting a layered structure (black) for (a) a hard-rock site (Pasadena Arts Center) and (b) a basin site (University of Southern California). Boxes show the middle 50th quantile of H/V ratio measurements at a particular period, with red bars showing the median. The lower and upper whiskers are at the 25th quantile minus 1.5 times the interquartile range (IQR) and the 75th plus 1.5 times the IQR, respectively, with remaining outliers shown as crosses. The dashed black lines show the predicted absolute H/V values from the Harvard Community Velocity Model (CVM-H).

Figure 5. V_S models, inverted using ZR/ZZ data, for depth ranges of (a) 0–500 m and (b) 500–1000 m. Inset plots show the Los Angeles basin area; note the different color scales for each subplot.

seismic arrays where the underlying crustal structure is less well known.

Inversion of 1D structure underneath a single station using either H/V values or phase-velocity is by necessity underdetermined. This is a consequence of the significant trade-offs between the three principle seismic parameters seen in the sensitivity kernels of Figure 1, for both H/V ratios and phase velocities. Removal of these trade-offs would require the calculation of phase-velocity dispersion curves for the stations using this study. Incorporation of these data would also extend the depth to which the inversion is sensi-

tive; however, there would also by necessity be some mapping of deeper structure into the shallow upper crust observed by H/V ratios, dependent on the relative weighting of datasets. Use of only H/V ratio measurements in an inversion for velocity structure is an illuminating exercise in that it is by physical necessity only sensitive to the near surface and consequently does not suffer the poorer depth resolution of phase-velocity measurements. Accurate assessment of the relative data uncertainty will be required for a future joint

7

Ⓔ

Erratum to

Rayleigh-Wave H/V via Noise Cross Correlation in Southern California

by Jack B. Muir and Victor C. Tsai

The authors would like to correct an error in the article by Muir and Tsai (2017). In the original article, a programming error resulted in the reported periods being incorrectly divided by 2.5, which is the Nyquist frequency of the data (5 Hz sample rate). Thus, to correct the results, all periods reported for data should be multiplied by 2.5; the period range of the article is consequently 2.5–37.5 s. This error does not change the qualitative conclusions of the article

—including the observation that the horizontal-to-vertical (H/V) data predict shallower effective basin depth—but does alter the quantitative conclusions of the article because the periods in the original article are 2.5 times too small. Note that the 10 s reported for Figure 1 is correct because this was a synthetic calculation. The change in periods necessitates recalculating the inversion results of Figures 4 and 5 and Ⓔ Figure S51 of the supplemental content; the corrected
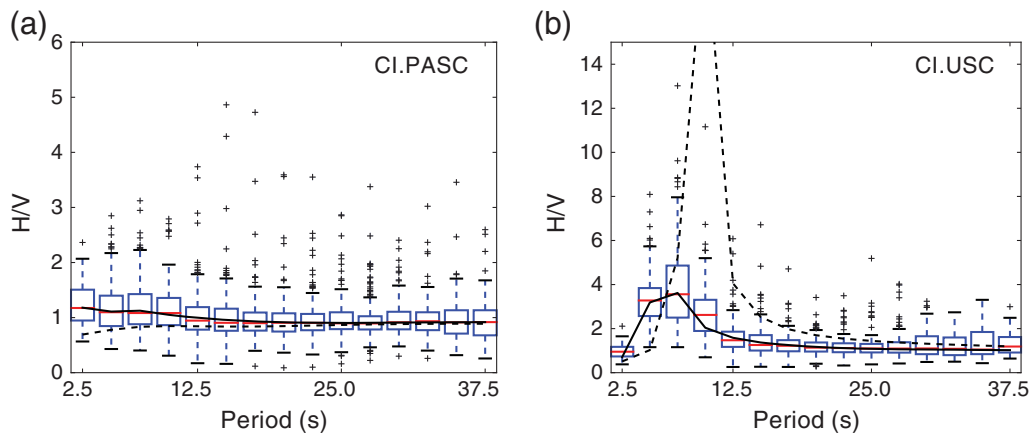

Figure 4. Example boxplots of horizontal-to-vertical (H/V) spectra with lines from fitting a layered structure (black) for (a) a hard-rock site (Pasadena Arts Center) and (b) a basin site (University of Southern California). Boxes show the middle 50th quantile of H/V ratio measurements at a particular period, with red bars showing the median. The lower and upper whiskers are at the 25th quantile minus 1.5 times the interquartile range (IQR) and the 75th plus 1.5 times the IQR, respectively, with remaining outliers shown as crosses. The dashed black lines show the predicted absolute H/V values from the Harvard Community Velocity Model (CVM-H).
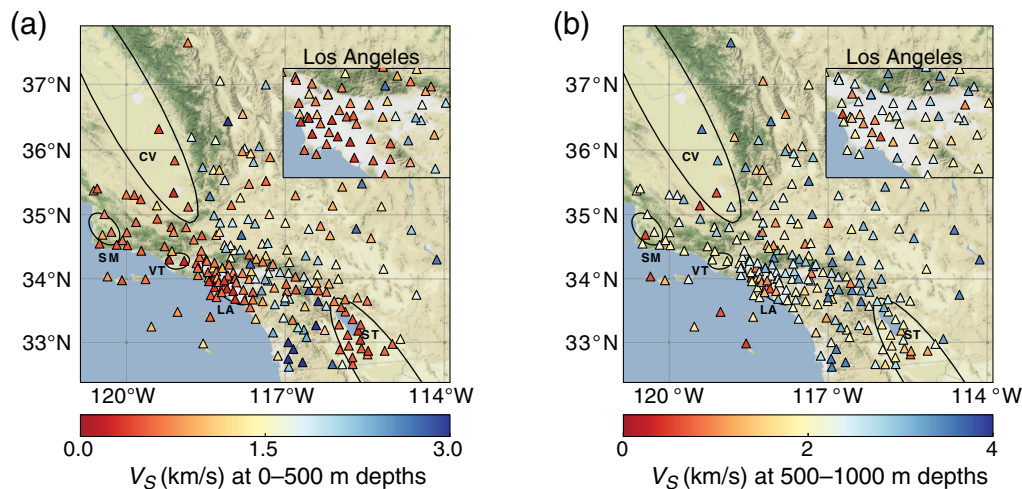

Figure 5. V_S models, inverted using ZR/ZZ data, for depth ranges of (a) 0–500 and (b) 500–1000 m. (Inset) Los Angeles basin area; note the different color scales for each subplot.

figures are supplied. In addition, for ease of use, we have supplied Ⓔ Tables S1, S2, and S3 with relabeled columns with the corrected periods and a corrected table caption noting that the standard deviations are of log H/V; these tables are otherwise unchanged.

Acknowledgments

Reference

Muir, J. B., and V. C. Tsai (2017). Rayleigh-wave H/V via noise cross correlation in southern California, *Bull. Seismol. Soc. Am.* **107,** no. 5, 2021–2027, doi: 10.1785/0120170051.

Division of Geological and Planetary Sciences
California Institute of Technology
Pasadena, California 91125 U.S.A.
jmuir@caltech.edu